Atomistic simulation of the surface structure of the TiO_2 polymorphs rutile and anatase

Peter M. Oliver,*† Graeme W. Watson, E. Toby Kelsey and Stephen C. Parker

Computational Solid State Chemistry Group, School of Chemistry, University of Bath, Claverton Down, Bath, UK BA2 7AY

Atomistic simulation has been used to calculate the surface structures and stability of the rutile and anatase polymorphs of TiO_2. The surface and attachment energies were used to evaluate the equilibrium and pseudo-kinetic morphologies. The surfaces expressed in rutile were {011}, {110}, {100} and {221} with surface energies of 1.85, 1.78, 2.08 and 2.02 J m^{-2} respectively. For anatase the {011} and {001} surfaces were dominant in the morphology with relaxed surface energies of 1.40 and 1.28 J m^{-2}. The predicted equilibrium forms were largely in good agreement with the reported experimental morphologies of rutile and anatase and showed the importance of surface relaxation.

Rutile is the most stable form of TiO_2 at ambient conditions with anatase metastable with respect to rutile. The surface properties of rutile have been the subject of numerous studies since the early 1970s when the decomposition of H_2O into hydrogen and oxygen in a photo-electrolysis cell was first reported.[1] This is particularly true of the TiO_2 {100} surface which has been studied experimentally[2–5] and theoretically.[6–10] Chung *et al.*[2] reported that argon-ion bombardment and annealing of the {100} surface at *ca.* 600, 800 and 1200 °C gave rise to three distinct structures, *i.e.* (1×3), (1×5) and (1×7) reconstructions. We have previously[11] modelled the (1×3) reconstruction of the {100} surface of TiO_2 and concluded that it was comprised of {110} facets in agreement with the LEED evidence.[4,5]

The surface properties of anatase have been studied less extensively. The surface dehydration of the {001} and {111} surfaces of anatase has been studied by Cordoba and Luque,[12] and they concluded that the {111} surface was most likely to be exposed. The morphological characteristics of authigenic rutile and anatase have been investigated by Morad[13] and these morphologies and those from other workers[14–16] will be used for comparison with the calculated morphologies later in this paper.

The aim of this paper is to provide reliable models for the surfaces of the low index planes of TiO_2 and to develop a strategy for ascertaining whether the models are reliable. The latter requires some independent check of the surface properties such as the crystal habit. Thus we are also concerned with using the energies from the final relaxed surfaces to determine whether the crystal growth of the polymorphs of TiO_2 is kinetically or thermodynamically controlled. This is achieved by considering the merits of evaluating the pseudo-kinetic and equilibrium forms and comparing them with available experiment. This is discussed later on, but first the methodologies used to calculate the equilibrium and pseudo-kinetic energies are described, followed by the generation of morphologies.

Methodology

The crystal is considered to be a series of charged planes lying parallel to the surface and periodic in two dimensions. The block is divided into two regions, region I and region II. The ions close to the surface in region I are explicitly relaxed whereas the ions in region II are held fixed. Thus during the minimisation process the ions in region I are allowed to relax relative to region II. The surface energies and structures of rutile and anatase were obtained using the computer code METADISE[17] developed to model dislocations, interfaces and surfaces.

The energy of the crystal is described *via* interatomic potentials. The potential is comprised of parametrised analytical expressions describing the interactions between atoms. The parameters used were developed by Matsui and Akoagi[18] (Table 1) and include electrostatic terms with short-range (9.6 Å) Buckingham potentials of the form shown in eqn. (1)

$$U_{r_{ij}} = \sum_{ij}{}' \frac{q_i q_j}{r_{ij}} + A_{ij}\exp(-r_{ij}/\rho_{ij}) - \frac{C_{ij}}{r_{ij}^6} \qquad (1)$$

where the charges of ions i and j, separated by a distance r_{ij}, are q_i and q_j, and A_{ij}, ρ_{ij} and C_{ij} are variable parameters fitted to the lattice properties such as elastic constants of rutile.

The Parry method,[19,20] a special case of the Ewald method,[21] was used to sum the electrostatic interactions by considering the crystal to be composed of a series of charged planes, of infinite size which terminate at a surface. This leads to three types of surfaces, as identified by Tasker.[22] In type I surfaces the stacking plane is neutral and is composed of both cations and anions in a stoichiometric ratio with no dipole perpendicular to the surface. Type II surfaces contain a series of charged planes making a repeat unit which has no dipole perpendicular to the surface. Type III surfaces are composed of alternately charged planes that produce a dipole perpendicular to the surface if cut between any plane. The Coulombic sum for such a surface cannot be evaluated as it is divergent.[23] If such surfaces are to be studied then the surface must be reconstructed such that the dipole is cancelled.[24] For example, the {111} surface of MgO is a type III surface and the simplest reconstruction is to remove half the surface plane making the surface layer 50% vacant. This cancels the dipole, enabling it to be simulated. The surface energy (γ_i) of a particular Miller index plane is calculated from the difference between the surface block simulation energy (U_{surf}) and the energy of the same number of bulk ions (U_{bulk}), *i.e.* surface excess energy, per unit area. Care is necessary to ensure that a sufficient number of layers are modelled so that the energy of the block has converged. The calculation of the

Table 1 Potential parameters for TiO_2

interaction	A/eV	ρ/Å	C/eV Å^6
$Ti^{2.196+}$–$O^{1.098-}$	16957.53	0.194	12.59
$Ti^{2.196+}$–$Ti^{2.196+}$	31120.2	0.154	5.25
$O^{1.098-}$–$O^{1.098-}$	11782.76	0.234	30.22

† Email: P.M. Oliver: p.m.oliver@bath.ac.uk

surface energy is given in eqn. (2)

$$\gamma_i = \left(\frac{U_{\text{surf}} - U_{\text{bulk}}}{\text{area}} \right) \quad (2)$$

In the calculation of the surface energy for a particular Miller index there may be multiple unique repeat units. If this is the case then each cut must be considered separately and the lowest energy cut used in the generation of the equilibrium morphology. This is further complicated by the presence of asymmetric cuts. A symmetric repeat unit $(hkl)_s$ has the same surface at the top and bottom. An asymmetric repeat unit $(hkl)_{as}$ has a different surface at the top and bottom. If the crystal space group has a centre of inversion, as is the case for rutile and anatase, then each asymmetric surface will have its own inverse $(hkl)_{asi}$ and the asymmetric cut is treated independently (Fig. 1).

Crystal morphology

The equilibrium shape of a crystal is that which minimises the total surface free energy, which at 0 K is approximated by the internal lattice energy. The relationship between equilibrium morphology and surface energy is most conveniently obtained from Wulff's theorem,[25] which is a corollary of an earlier theorem by Gibbs.[26] Gibbs proposed that the equilibrium form of a crystal should possess a minimum (free) energy for a given volume and is shown in eqn. (3)

$$E_{\text{surf}} = \sum_i \gamma_i \phi_i = \text{minimum for constant volume} \quad (3)$$

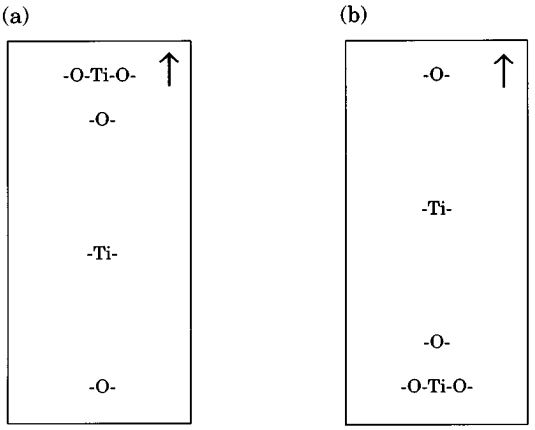

Fig. 1 Stacking sequence illustrating asymmetric surface (as) and asymmetric surface-inverse (asi) for the (a) {111a}-as and (b) {111b}-asi of rutile

where γ_i and ϕ_i are the specific surface energy and surface area of the ith crystallographic face. The crystal morphology is the shape which describes a minimum volume from a polar plot of surface energy as a function of orientation, *i.e.* the height of a face is proportional to its surface energy. This was later proved using both geometric[27–29] and thermodynamic arguments.[30,31] This approach works best for small crystals, but for large crystals the morphology is best described using a kinetic treatment. Two straightforward phenomenological models which attempt to incorporate these kinetic factors are the Donnay Harker scheme[32] and that of Hartman and Bennema.[33] These are briefly described below.

The Donnay Harker methodology,[32] which attempts to model the rate of growth, applies the relation shown in eqn. (4)

$$\text{height} \propto \frac{1}{d_{hkl}} \quad (4)$$

where d_{hkl} is the repeat distance for Miller index $\{hkl\}$ and the height is the length of the normal to the face in the Wulff plot.

The attachment energy used in the Hartman and Bennema model[33] is the energy per atom released for face (hkl) when a new slice of thickness d_{hkl} crystallises on it and is used to model the rate of growth. The thickness d_{hkl} is the minimum slice which will repeat the same surface configuration. When evaluating the pseudo-kinetic morphology from the attachment energies the lowest attachment energy is used. The length of the normal is proportional to the attachment energy[34] thus

$$\text{height} \propto U_{\text{attach}(hkl)} \quad (5)$$

where U_{attach} is the attachment energy for surface (hkl).

In the next section the morphologies generated using the above methodologies are compared and contrasted.

Structure and morphology of rutile and anatase

Rutile is tetragonal ($a = b \neq c$, $P4_2/mnm$)[35] with Ti^{4+} surrounded by six O^{2-} at the corners of a slightly distorted octahedron and each O^{2-} surrounded by three Ti^{4+} lying in a plane at the corners of an equilateral triangle. Anatase is also tetragonal ($a = b \neq c$, $I4/amd$)[35] and has the same coordination as rutile. The structural difference between these two polymorphs is in how the octahedra are connected. Rutile is comprised of linear chains of edge-sharing octahedra where the chains themselves are connected by the octahedra corners. The anatase structure comprises of two interpenetrating zigzag chains of edge-shared octahedra which are linked to form a three-dimensional network of edge-shared octahedra.

All surface planes up to index 2 were considered for rutile and anatase. The low index planes were chosen as they are in

Table 2 Surface characteristics and energies (before and after relaxation) for rutile showing the area, repeat distance, unrelaxed and relaxed surface energies, attachment energy, symmetry and type of surface

$\{hkl\}$	area/Å^2	d_{rep}[a]/Å	E_{unrel}[b]/J m^{-2}	E_{rel}[c]/J m^{-2}	E_{attach}/eV	symmetry[d]	type[e]
{011b}	38.79	3.51	2.71	2.18	−0.54	s	II
{011a}			1.60	1.40	−0.32	s	II
{001}	14.22	2.39	1.28	1.28	−0.37	s	II
{112}	58.42	2.33	2.05	1.81	−0.63	s	II
{100}	36.09	1.89	2.26	1.68	−1.02	s	II
{121b}	81.94	1.66	2.42	1.94	−2.21	s	II
{121a}			4.96	3.05	−5.35	s	II
{012}	45.94	1.48	4.76	2.42	−3.10	s	II
{110}	51.03	1.34	2.65	2.19	−1.57	s	II
{021b}	73.56	0.93	2.36	1.81	−1.12	s	II
{021a}			5.91	2.97	−3.91	s	II
{120}	80.69	0.84	2.54	1.98	−1.61	s	II
{122}	85.56	0.79	4.98	2.05	−4.50	s	II
{111}	52.98	0.64	5.75	2.87	−5.20	s	II
{221}	103.05	0.33	4.89	2.69	−8.10	s	II

[a]Repeat distance. [b]Unrelaxed, [c]relaxed surface energy. [d]s = Symmetric surface. [e]Tasker classification.

Table 3 Surface characteristics and energies (before and after minimisation) for anatase showing the area, repeat distance, unrelaxed and relaxed surface energies, attachment energy, symmetry and type of surface

{*hkl*}	area/Å^2	d_{hkl}/Å	E_{unrel}[a]/J m^{-2}	E_{rel}[b]/J m^{-2}	E_{attach}/eV	symmetry[c]	type[d]
{110}	19.12	3.18	2.05	1.78	−0.42	s	II
{011}	24.30	2.50	2.06	1.85	−0.50	s	II
{100}	13.52	2.25	2.40	2.08	−0.64	s	II
{111b}	27.81	2.18	3.95	2.60	−1.22	asi (a)	II
{111a}			3.95	2.91	−1.22	as	II
{120b}	30.23	2.01	6.13	2.62	−2.45	asi (a)	II
{120a}			6.13	3.66	−2.45	as	II
{121}	36.35	1.67	2.67	2.16	−1.11	s	II
{001}	20.19	1.50	2.81	2.40	−1.40	s	I
{221a}	43.24	1.4	3.83	2.02	−1.78	as	II
{221b}			3.83	3.29	−1.78	asi (a)	II
{112}	44.68	1.36	4.88	4.01	−3.04	s	II
{122b}	50.44	1.20	4.01	2.52	−2.36	asi (a)	II
{122a}			4.01	2.82	−2.36	as	II
{021}	33.75	0.90	2.85	2.28	−1.61	s	II
{012}	42.58	0.72	6.06	2.95	−5.10	s	I

[a]Unrelaxed, [b]relaxed surface energy. [c]s = Symmetric surface, as = asymmetric surface, asi(a) = asymmetric inverse of the asymmetric surface a. [d]Tasker classification.

general the most stable and to provide some limits to the computational search. The surface energies are summarised in Tables 2 and 3.

The equilibrium morphology is compared with experiment, the Donnay Harker scheme and the attachment energy scheme in Fig. 2 and 3 for rutile and anatase, respectively. The pseudo-kinetic morphologies of rutile calculated using the Donnay Harker (DH) [Fig. 2(a)] and attachment energy (AE) [Fig. 2(b)] schemes are very similar with only the {011} and {110} surfaces expressed. This is contrary to the observed morphology[14,15] [Fig. 2(e)]. The unrelaxed equilibrium morphology [Fig. 2(c)] includes the {100} surface and shows closer agreement. However, the best agreement is obtained by using the relaxed surface energies generating a morphology expressing the {011}, {110}, {100} and {221} faces [Fig. 2(d)]. For all of the calculated morphologies the {011} surface is too stable resulting in a squashed habit. These results indicate that surface relaxation plays an important role in determining

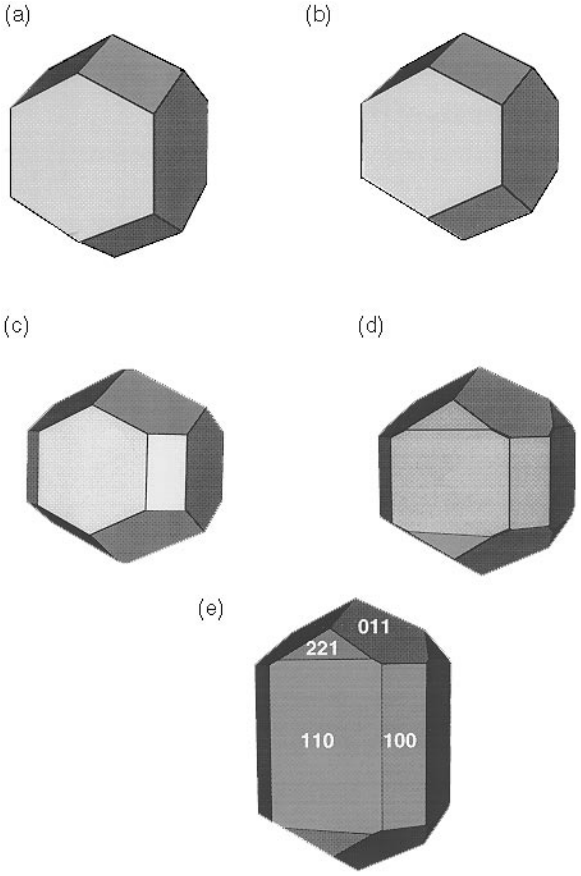

Fig. 2 The calculated and experimental morphology of rutile (a) Donnay Harker, (b) attachment energy, (c) before minimisation, (d) after minimisation, (e) experimental[15]

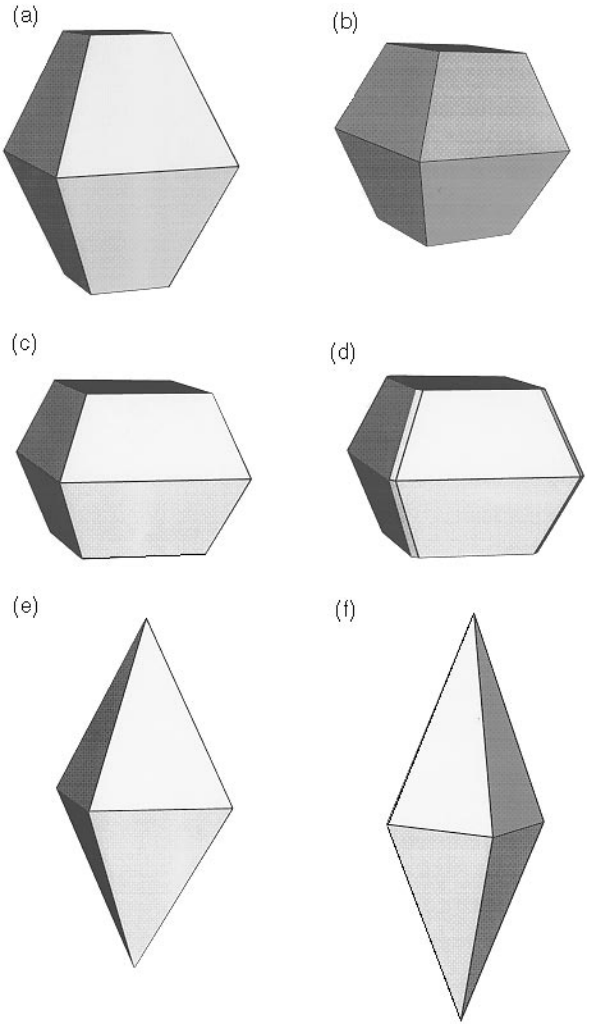

Fig. 3 The calculated and experimental morphology of anatase (a) Donnay Harker, (b) attachment energy, (c) before minimisation, (d) after minimisation, (e) experimental {011},[15] (f) experimental {111}[16]

which faces are expressed and thus schemes that omit surface relaxation are disadvantaged. These results compare well to the electronic structure calculations of Ramamoorthy *et al.*[9] Their calculations incorrectly predicted the inclusion of the {001} surface leading to a capped morphology. In addition the atomistic approach allowed us to investigate index 2 surfaces which were beyond the scope of the electronic structure calculations, and the {221} surface was identified as being in the calculated morphology. This is apparently a discrepancy as the {111} face is commonly identified in this position. However, both are first-order dipyramids of the tetragonal system and thus would appear very similar, especially since the faces are present with very small surface areas. This leads to the prediction that the previously identified {111} surfaces may in fact be {221}.

On simulating anatase the unrelaxed equilibrium, DH and AE morphologies all expressed the {001} surface, contrary to the experimentally reported morphology, resulting in a capped {011} octahedral habit (Fig. 3). Upon relaxation the morphology hardly changes with the slight expression of the {112} face. Both experimental morphologies show an octahedral habit but there is some ambiguity as to whether this is due to {011}[15] [Fig. 3(e)] or {111} [Fig. 3(f)] faces.[16] This study suggests that the octahedra are formed from {011} faces and that they appear as {011} octahedra capped with {001} faces. Although the {001} surface is not present in the experimental morphology[15] the {001} is a major cleavage plane for anatase, identifying it as a stable surface which is reflected in its low surface energy.

Relaxed surface structure of rutile and anatase

One very important advantage that energy minimisation has over the DH and AE schemes is that the atomic structure and relaxations of ions at the surface can be examined. The surface structures after minimisation for the two most stable surfaces of rutile, the {110} and {011}, are given in Plate 1(a) and (b).

The {110} surface [Plate 1(a)] is comprised of two-coordinate oxygen ions in the [001] direction bonded to the six-coordinate titanium ions which alternate with five-coordinate titanium ions in the [$\bar{1}$10] direction. This can be envisaged as cleaving between the chains of octahedra. Upon relaxation the surface energy decreased from 2.05 to 1.78 J m^{-2}. On this surface the first layer surface bridging oxygen ions relaxed 0.08 Å into the surface. On the second layer the six- and five-coordinate titanium ions moved outward and inward by 0.25 Å and the second layer oxygens moved outward slightly by 0.02 Å. In comparison to electronic structure calculations[8,9] the agreement is good, but in their study the amplitudes of the relaxations are less with the second layer six- and five-coordinate titanium ions moving 0.1 Å. This discrepancy (as the authors point out) could be because their five-layer slab is not completely converged.

The {011} surface is comprised of rows of oxygen ions in the [0 $\bar{1}$0 4] direction bonded to five-coordinate titanium ions and can be envisaged as cleaving through the linear chains of octahedra. The surface energy of the {011} surface of 2.06 J m^{-2} before relaxation is very similar to that of the {110} surface. However, after relaxation the surface is slightly less stable than the {011} by 0.07 J m^{-2} with a surface energy of 1.85 J m^{-2}. For this surface the relaxation is small which agrees with previous electronic structure calculations.[10] The surface oxygen ions relaxed 0.02 Å out of the surface and the second layer of oxygen ions relaxed 0.01 Å into the surface. Similarly the relaxations of the titanium ions is small, with their displacement being 0.01 Å out of to the surface on the first layer and in subsequent layers they did not move.

The relaxations for the two stable surfaces of anatase, {001} and {011}, with relaxed surface energies of 1.28 and 1.40 J m^{-2} respectively, are given in Plate 2(a) and (b). The {001} surface is composed of a surface layer of oxygen ions which are two-coordinate in the [010] direction. The five-coordinate titanium ions bonded to these oxygen ions are themselves bonded to three-coordinate oxygen ions in the [100] direction. The surface energies before and after relaxation for the {001} surface of anatase are identical, indicating that this is a very stable surface. From the perspective of the linked octahedra this surface is generated by cleaving between the interpenetrating octahedral chains, which may account for its stability. This is reflected in the relaxed positions of the ions. The first layer

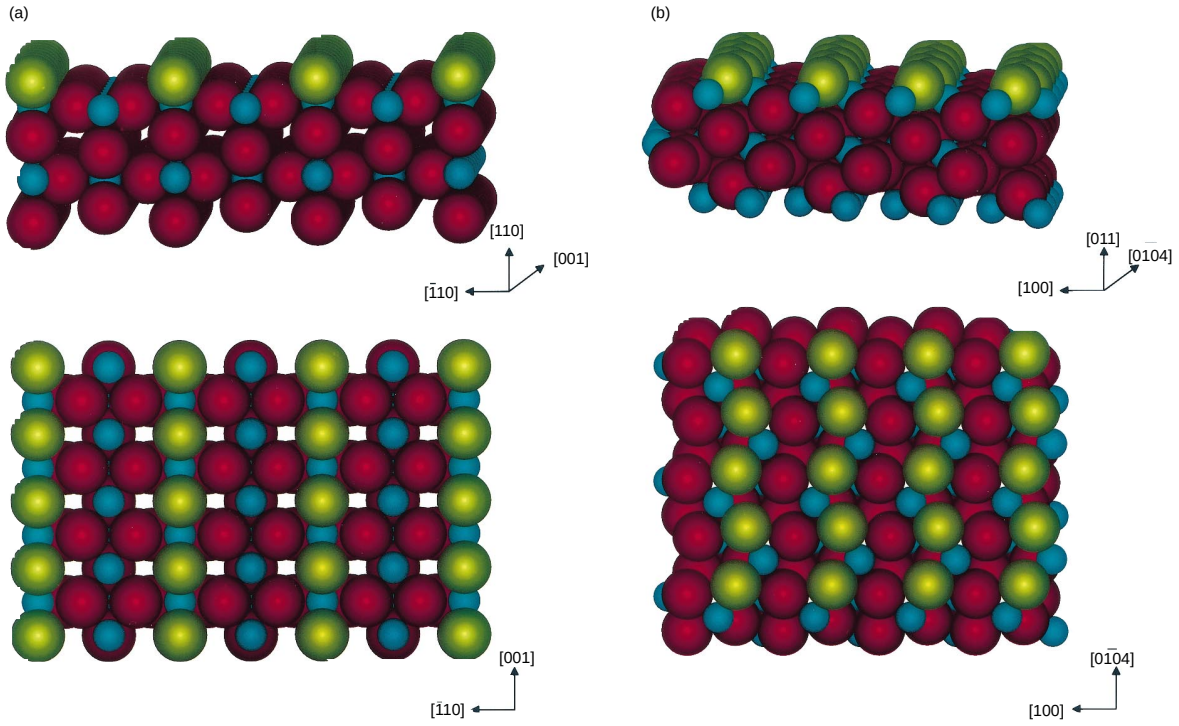

Plate 1 The relaxed surface structure (top and side views) of rutile (a) {110} and (b) {011}. The surface oxygen ions are yellow, bulk oxygens red and titanium ions blue.

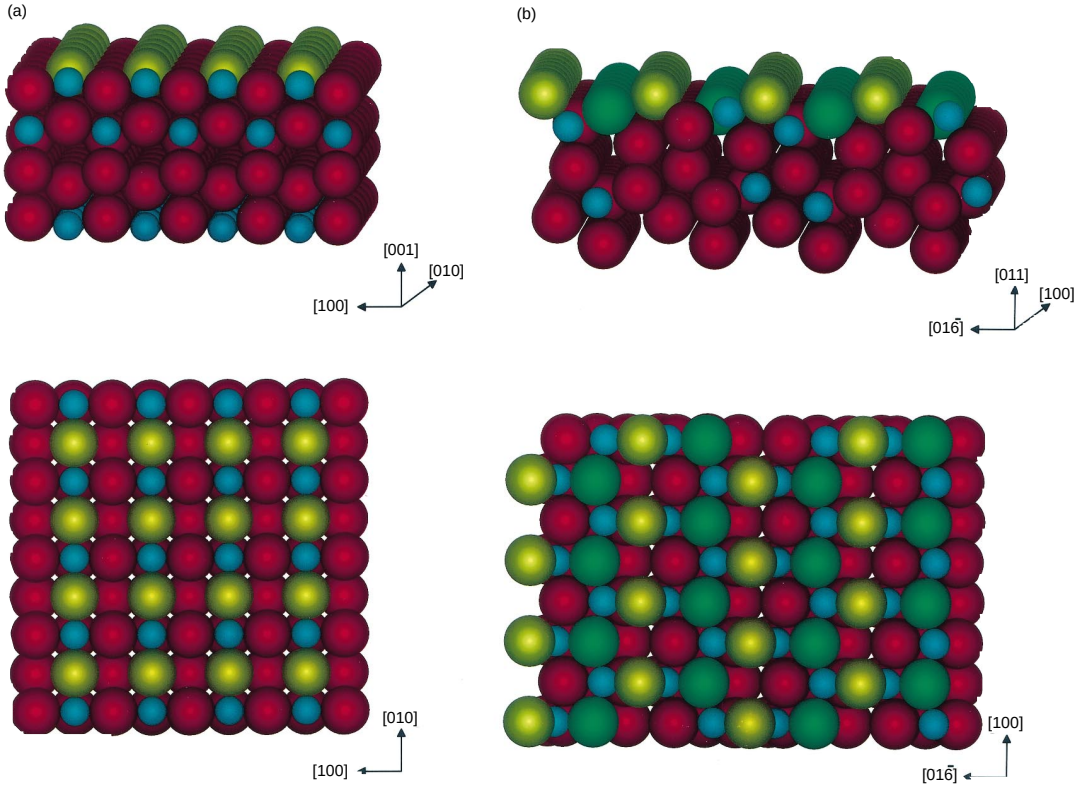

Plate 2 The relaxed surface structure (top and side views) of anatase (a) {001} and (b) {011}. The surface oxygen ions are yellow, second layer oxygen ion green, bulk oxygens red and titanium ions blue.

oxygen ions moved 0.04 Å into the surface and the five-coordinate titanium ions moved by 0.01 Å out of the surface. This is in contrast to the {001} surface of rutile where the surface contains four-coordinate titanium ions and is correspondingly less stable with a surface energy of 2.40 J m^{-2}.

The {011} surface anatase is composed of rows of oxygen ions in the [100] direction two-coordinated to five-coordinate titanium ions in the second layer in the [01$\bar{6}$] direction. These titanium ions are themselves bonded to three-coordinate oxygen ions in the [100] direction. The {011} surface can be envisaged as cleaving through the interpenetrating chains which are inclined to the surface normal. In contrast to the {001} surface the relaxations on the {011} surface were larger, the first layer oxygen ions moved 0.08 Å into of the surface and the second layer oxygen ions 0.15 Å out of the surface. The titanium ions moved relatively little with displacements of 0.02 Å for the five-coordinate titanium into the surface and 0.03 Å out of the surface for the six-coordinate surface titanium ions.

Conclusions

The morphologies of rutile and anatase have been calculated using equilibrium and pseudo-kinetic methodologies and in general agree with those observed experimentally. The four surfaces expressed in the relaxed equilibrium morphology of rutile, {011}, {110}, {100} and {221} with surface energies of 1.85, 1.78, 2.08 and 2.02 J m^{-2}, are in good agreement with experiment and with electronic structure calculations. This indicates that surface relaxation is important for determining morphology because neither the Donnay Harker nor the attachment energy schemes achieved this level of agreement. For anatase the {011} and {001} surfaces were dominant in the morphology with relaxed surface energies of 1.40 and 1.28 J m^2. The most stable surface of rutile, the {110}, contains five- and six-coordinate species at the surface and for the most stable surface of anatase, the {001}, five-coordinate species are found at the surface, which in part may be the source of the different reactivities and surface properties.

We would like to thank the EPSRC for funding and Molecular Simulations Inc. for the provision of INSIGHT II.

References

1 A. Fujishima and K. Honda, *Nature (London)*, 1972, **238**, 37.
2 Y. W. Chung, W. J. Lo and G. A. Somorjai, *Surf. Sci.*, 1977, **64**, 588.
3 C. A. Muryn, P. J. Hardman, J. J. Crouch, G. N. Raiker, G. Thornton and D. S. L. Law, *Surf. Sci.*, 1991, **251/252**, 747.
4 P. Zschack, J. B. Cohen and Y. W. Chung, *Surf. Sci.*, 1992, **262**, 395.
5 P. W. Murray, F. M. Leibsle, H. J. Fisher, C. F. Flipse, C. A. Muryn and G. Thornton, *Phys. Rev. B*, 1992, **46**, 12877.
6 R. V. Kasowski and R. H. Tait, *Phys. Rev. B*, 1992, **20**, 5168.
7 M. Tsukada, C. Satoko and H. Adachi, *J. Phys. Soc. Jpn.*, 1979, **47**, 1610.
8 M. Ramamoorthy, R. D. King-Smith and D. Vanderbilt, *Phys. Rev. B*, 1994, **49**, 7709.
9 M. Ramamoorthy, D. Vanderbilt and R. D. King-Smith, *Phys. Rev. B*, 1994, **49**, 16723.
10 S. Munnix and M. Schmeits, *Phys. Rev. B*, 1984, **30**, 2202.
11 P. M. Oliver, S. C. Parker, J. Purton and D. W. Bullett, *Surf. Sci.*, 1994, **307–309**, 1200.
12 A. Cordoba and J. J. Luque, *Phys. Rev. B*, 1985, **31**, 8111.
13 S. Morad, *Sedimentary Geology*, 1986, **46**, 77.
14 W. E. Ford and E. S. Dana, *A Textbook of Mineralogy*, Wiley, Chichester, 1958, 4th edn.
15 I. Kostov, *Mineralogy*, Nauka i Izkustvo, Sofia, 1968.
16 G. Munuera, F. Moreno and F. Gonzalez, *Reactivity of Solids*, ed. J. S. Anderson, M. W. Roberts and F. S. Stone, Chapman and Hall, London, 1972.
17 G. W. Watson, E. T. Kelsey, N. H. de Leeuw, D. J. Harris and S. C. Parker, *J. Chem. Soc., Faraday Trans.*, 1996, **92**, 433.
18 M. Matsui and M. Akoagi, *Molecular Simulation*, 1991, **6**, 239.
19 D. E. Parry, *Surf. Sci.*, 1975, **49**, 433.
20 D. E. Parry, *Surf. Sci.*, 1976, **54**, 195.
21 P. P. Ewald, *Ann. Phys.*, 1921, **64**, 253.
22 P. W. Tasker, *J. Phys. C: Solid State Phys.*, 1979, **12**, 4977.
23 F. Bertaut, *Compt. Rend.*, 1958, **246**, 3447.

24 P. M. Oliver, S. C. Parker and W. C. Mackrodt, *Modelling Simul. Mater. Sci. Eng*., 1993, **1**, 755.
25 G. Wulff, *Z. Kristallogr. Kristallgeom*., 1901, **39**, 449.
26 J. W. Gibbs, *Collected Works*, Longman, New York, 1928.
27 H. Hilton, *Mathematical Crystallography*, Oxford, 1903.
28 H. Leibman, *Z. Kristallogr*., 1914, **53**, 171.
29 M. von Laue, *Z. Kristallogr*., 1943, **105**, 124.
30 I. N. Stranski, *Z. Phys. Chem. B*, 1938, **38**, 451.
31 M. Volmer, *Kinetik der Phasenbildung*, Steinkopff, Leipzig, 1939.
32 J. D. Donnay and G. Harker, *Am. Mineral*., 1937, **22**, 446.
33 P. Hartman and F. Bennema, *J. Crystal Growth*, 1980, **49**, 145.
34 C. F. Woensdregt, *Faraday Discuss*., 1993, **95**, 97.
35 W. A. Deer, R. A. Howie and J. Zussman, *Rock Forming Minerals*, Longmans, London, 1962, 1st edn., vol. 5.

Paper 6/06353E; *Received* 16*th September*, 1996